Photoinduced transformations of Acid Violet 7 and Acid Green 25 in the presence of TiO2 suspension.

(Article begins on next page)

10 April 2024

UNIVERSITÀ DEGLI STUDI DI TORINO

Photoinduced transformations of Acid Violet 7 and Acid Green 25 in the presence of TiO₂ suspension

D. Fabbri, P. Calza*, A. Bianco Prevot

Dipartimento di Chimica Analitica, Università di Torino, via P. Giuria, 5. 10125 Torino, Italy

*corresponding author. Phone: +390116707626; fax: +390116707615; e-mail:
paola.calza@unito.it

Abstract

An azo dye (Acid Violet 7) and an anthraquinone dye (Acid Green 25) were degraded in aqueous solution using titanium dioxide as photocatalyst. Their fate was studied through dyes decomposition, identification of the main and secondary transformation products and assessment of mineralization. Carbon complete mineralization was achieved in both cases together with the total conversion of the sulphonic groups into sulphate ions; nitrogen was recovered as nitrate and ammonium ions.

The transformation intermediate products were identified by means of HPLC/MS and GC/MS techniques. Acid Violet 7 transformation involved the detachment of sulphonic group, hydroxylation, and detachment of the amino acetic moiety, with the formation of hydroxyl naphthalene. Conversely, Acid Green 25 transformation proceeded through the formation of 18 initial compounds and involved the detachment of one (or two) sulphonic groups and/or hydroxylation, followed by the detachment of the benzene ring.

Keywords: azo dyes, antraquinone dye, transformation products, HPLC/MS, TiO₂

Introduction

Among synthetic compounds of possible environmental concern, dyes represent a very important category, because of their extensive, widespread use. They find application in many fields (photochemical, textile, photographic, foodstuffs, etc...) thus causing their presence in wastes to be carefully considered. Besides classical waste waters treatment (flocculation, adsorption on active carbon) not even biological degradation was effective in their elimination, the efficiency largely depending on the dye structure. Moreover, biodegradation of dyes is in general not efficient enough, due to the presence of complex and stable aromatic structures. For these reason an increasing appeal grew for the use of advanced oxidation processes in order to obtain the complete abatement of dyes and possibly the mineralization of the organic carbon. Among these technologies, TiO_2 mediated photo-catalysis has been demonstrated to be efficient in decolorize dye effluent in the presence of UV-Vis light. Many papers in the last years dealt in particularly with the TiO_2 assisted degradation of anthraquinone, quinoline and azo dyes [1-14], showing good results in both dye bleaching and mineralization. The optimization of dyes degradation by mean of AOT's was also considered in terms of chemometric methods such as response surface methodology (RSM) based on statistical design of experiments (DOEs). This kind of approach accounts for possible interaction effects between the experimental parameters and could represent a powerful tool in order to determine, with a relatively low number of experiments, the experimental conditions yielding to the optimum of the process [15-17].

The reactions taking place when an aqueous suspension of TiO_2 is irradiated at a wavelength above 380 nm have been widely discussed in the literature [18-19]. As far the mechanism of organic compounds degradation is concerned, it has been suggested that the hydroxyl radicals and superoxide radical anions are the primary oxidizing species in the photocatalytic oxidation processes. These oxidative reactions would result in the bleaching of the dye. Alternatively, direct absorption of light by the dye can lead to charge injection from the excited state of the dye to the conduction band of the semiconductor, as summarized in Eqns 1 and 2:

$$Dye_{ads} + h\nu \rightarrow Dye^*_{ads} \qquad (1)$$
$$Dye^*_{ads} + TiO_2 \rightarrow Dye_{ads} + TiO_2(e^-) \qquad (2)$$

There are several classes of dyes that do not favour donation from excited states, such as anthraquinone dyes, because of the presence of two electron-withdrawing carbonyl groups which are susceptible to accept, rather than donate, an electron.

Among the different dye families, azo and anthraquinone dyes are the mostly used for industrial purposes. Azo-dyes cover about one-half of the dyes employed in the textile industry and are structurally characterized by the presence of one or more azo bonds; their degradation by means of TiO_2 photocatalysis has been recently reviewed [20]. Anthraquinone dyes correspond to the second most important class of commercial dyes after azo compounds and are mainly used for dyeing polyamides, leather and wool [21]. The photocatalytic degradation of anthraquinone dyes has been studied by several groups [22]; even if all the investigated structures showed a fast bleaching, complete mineralization was not observed in short irradiation times, due to the stability of the anthraquinone moiety.

Depending on the chromogenes, chromophores and auxochromes, dyes exhibit different physical and chemical properties, such as water solubility, colour, brightness and light absorption characteristics. The existence of a conjugated system increases the stability toward photocatalytic treatment, as assessed by the enhancement in the photo-stability shown at the increasing of the number of aromatic rings. In particular, as regards azo dyes the structures not adjacent to azo bond shown higher reactivity but lower decolourization rate at the increasing number of azo groups [23].

The present research deals with the photocatalytic degradation of Acid green 25 (AG25), an anthraquinone dye, and Acid Violet (AV7), an azo dye. The TiO_2 mediated photodegradation of AG25 was previously considered [24], but no particular attention was devoted to the identification of intermediates and final products. With regard to AV7, previous studies demonstrate the feasibility of its decolourization through biodegradation using *pseudomonas putida* [25]; the transformation proceeds through an azo-reduction, with the formation of toxic compounds [26]. Moreover, the mineralization process was investigated with Fenton reaction, but no studies exist about its abiotic transformation products [27].

We have focused our study mainly on the assessment of the degradation of the two dyes, the identification of intermediate products as well as the evaluation of the mineralization process. For this reason, powerful analytical techniques such as gas and liquid chromatography coupled to mass-spectrometry and ion chromatography were employed. The use of GC-MS technique to identify intermediates coming from the photocatalytic degradation of azo dyes has been documented [28, 29]. Nevertheless, a lack of information exists about the possible formation of hydrophilic intermediates, still containing the chromophore groups, which cannot be efficiently extracted in the solvents typically used in GC/MS analysis. In these cases, an help on the identification can arise from the use of HPLC/MS technique [30, 31], since it allows the direct analysis of polar compounds, requiring neither derivatization nor complex extraction procedures.

2. Experimental section

2.1. Material and reagents

Acid Violet 7 (purity >50%) and Acid Green 25 (purity >75%) were purchased from Aldrich. HPLC grade water was obtained from MilliQ System Academic (Waters, Millipore). HPLC grade acetonitrile (BDH) was filtered through a 0.45 μm filter before use. Tetraethylbromamine reagent grade was purchased from Carlo Erba. Experiments were carried out using TiO_2 Degussa P25 as the photocatalyst.

2.2. Irradiation procedures

The irradiation experiments were carried out in Pyrex glass cells, filled with 5 ml of a suspension containing the dye (20 mg/L) and TiO_2 (200 mg/L) in air saturated conditions. The illumination was performed using a Blacklit Philips TLK/05 40 Watt lamp with the maxima emission at 360 nm. The temperature reached during the irradiation was $38 \pm 2°C$. The entire content of each cell was filtered through a 0.45 μm filter and then analyzed by the appropriate technique.

2.3. Analytical procedures

2.3.1. Liquid Chromatography

The chromatographic separations followed by a MS analysis were run on Thermo Finnigan instrument using a C18 column Lichrosphere, 250×4.0 mm. Injection volume was 20 μL and flow rate 1000 μL/min. Gradient mobile phase composition was adopted: 100/0 to 50/50 in 14 min ammonium acetate 0.05% / acetonitrile.

A Surveyor mass spectrometer (Thermo Finnigan) equipped with an atmospheric pressure interface and an ESI ion source was used. The LC column effluent was delivered into the ion source using nitrogen as both sheath and auxiliary gas. The cone voltage was set at 30, 70 and 100 volts value. The heated capillary value was maintained at 300°C. The acquisition method used was previously optimized in the tuning sections for the parent compound (capillary, magnetic lenses and collimating octapoles voltages) in order to achieve the maximum of sensitivity. The tuning parameters adopted for ESI source have been the following: capillary voltage 2.5 V, RF Lens Bios 0.3 V, ion energy 1V. Mass spectra were collected in full scan negative mode in the range 50-900 m/z.

50 ml of AG25 and AV7 samples subjected to 10 min of irradiation were concentrated to 1 ml in a Bruker lyophilizer and analyzed by HPLC/MS by applying different cone voltages.

2.3.2. GC/MS

A GC/MS spectrometer (Agilent 6890, series II) equipped with a 5% phenylmethylpolysiloxane column (Agilent HP-5; 30 m x 0.25 mm) was used. The GC operating parameters were as follows: injector at 300°C, splitless injection (1 min), volume injected 1 μl. The analyses were performed using a double gradient. Temperature was linearly increased at 10 °C/min from 50 to 250 °C and then was brought to 300 °C at a rate of 20°C/min. Prior to GC/MS analysis, samples subjected to 10 and 30 min of irradiation were extracted with dichloromethane and concentrated to 100 μl in a Rotavapor.

2.3.3. Ion chromatography

A Dionex instrument was employed equipped with a conductimetric detector. Determination of ammonium ions was achieved using a CS12A column and 25 mM metansulphonic acid as eluant, at a flow rate of 1 mL/min. In these conditions the retention time for ammonium ion was 4.7 min. The anions were analyzed using an AS9HC anionic column, 10 mM $NaHCO_3$ and 4 mM K_2CO_3 as eluant and a flow rate of 1 mL/min. In these experimental conditions the retention time of nitrate and sulphate were 8.90 and 13.68 min, respectively.

2.3.4. Total organic carbon analyzer

Total organic carbon (TOC) was measured on filtered suspensions using a Shimadzu TOC-5000 analyzer (catalytic oxidation on Pt at 680 °C). The calibration was performed using standards of potassium phthalate.

3. Results and discussion

3.1. Dyes photolysis and photocatalytized degradation

Preliminary experiments were carried out to evaluate the extent of hydrolysis and photolysis on the dyes transformation. Dark experiments showed that adsorption on the catalyst can be disregarded for both dyes. Conversely, upon light exposure the dyes photo-bleaching occurred; as

displayed in Figures 2 and 3, after a time period of 120 min, 20% and 92% of AG25 and AV7 respectively were degraded. In the presence of TiO_2 200 mg/L more rapid degradation was observed, with a kinetic profile following a first order law. Results obtained by direct photolysis proved that for AG25 the photolysis process was scarcely responsible for the observed fast transformations when the solution was irradiated in the presence of the photocatalyst (see Figure 2). Conversely, for AV7 direct photolysis contributed to the dye disappearance ($t_{1/2}$ 45 min, see Figure 3) but not to the dye mineralization; in the considered irradiation times, the TOC content was steady.

Looking closer to the photocatalytic process, the concentration abatement for both dyes occurred with an half-life of 5 min and photo-bleaching curves showed a comparable rate. More in details, while AG25 photo-bleaching closely matched the dye disappearance curve, photo-bleaching curve for AV7 showed a increased half-life time ($t_{1/2}$=10 min), compatible with the formation of still coloured intermediate compounds.

3.2. Transformation products

The study of the dyes transformation products was performed by HPLC/MS and GC/MS. Negative-ion electrospray ionization is the most suitable ionization technique for the molecular mass determination of polysulphonated dyes or other dyes carrying a negative charge [32]. For such, analyses by HPLC/MS were run in the ESI negative mode, which appears to be more sensitive and suitable for most of the transformation products. The negative-ion ESI mass spectra of polysulphonic acids provided a simple means for the determination of the molecular mass and of the number of acid groups. As a matter of fact such compounds exhibit typical mass spectra of singly deprotonated molecules (negative ions) with *m/z* values corresponding to the presence of as many sodium ions as acid groups but the deprotonated one.

3.2.1. AG25 transformation products

AG25 transformation proceeded through the formation of 19 main intermediate compounds, whose *m/z* ratios, product ions and retention times are collected in Tables 1 and 2. The proposed structures are consistent with the fragmentation profiles of their deprotonated forms, as will be described in details below.

Four products with a nominal mass of 594 Da and detected in its deprotonated form at *m/z* 593 can be postulated to be formed via an AG25 hydroxylation. All the four isobaric species formed two

product ions at *m/z* 615 (sodium adduct [M+Na]⁻) and *m/z* 296 (bicharged ion). The spectra obtained at different cone voltages for 593-A and 593-B only showed the formation of these two product ions, so that no considerations can be done about the position for the OH attack. Conversely, additional product ions were formed in 593-C and D MS spectra. 593-C eliminated toluene sulphonic acid, as shown in Figure 4. 593-D afforded a product ion at *m/z* 591, well-matched with the hydroxylation on a position where a keto/enolic equilibrium can took place, i.e in ortho position.

Two transformation products at *m/z* 611 were formed and attributed to the bihydroxy AG25 derivatives. Again, both derivatives showed the formation as product ions of the sodium adduct at *m/z* 633 and the bicharged ion at *m/z* 305. In addition, 611-A afforded methanol elimination (product ion at *m/z* 579), so signifying the possible location of one (of the two) OH group on the methyl group.

Five transformation products at *m/z* 513 were detected, whose formation could involve:

    (1) the detachment of SO_2 or;

    (2) the detachment of SO_3^- and the insertion of an OH group;

    (3) the detachment of SO_3^-, demethylation and the oxidation of a methyl group to an aldehydic group.

The isomer 513-B followed the second transformation route, while the isomer 513-C was subjected to the latter transformation as comes up by Scheme 1.

The isomer 513-B yielded several structurally-diagnostic product ions that arise from: (I) the detachment of a methylaminobenzene sulphonic acid molecule, with the formation of a product ion at *m/z* 328; it permitted to exclude the involvement of this moiety in the transformation process; (ii) a methyl aniline loss, with the formation of a product ion at *m/z* 408 and its sodium adduct (*m/z* 430). We can then conclude that the benzene ring was subjected to desulphonation but not hydroxylation, that was confined to the anthraquinone moiety.

The structural isomer 513-C eliminated a benzene molecule with the formation of a product ion at *m/z* 435. Therefore, both the demethylation and desulphonation likely took place at the same benzene ring, with the formation of the structure shown in Scheme 1. For the 513-D any product ions were formed, even at high cone voltage. 513-E easily loses a water molecule (product ion at *m/z* 495).

Four structural isomers at *m/z* 531 were identified and attributed to the bihydroxylated/demethylated and desulphonated AG25 derivatives. The key fragmentation pathway followed by 531 A is shown in Scheme 2.

531-A showed a product ion at *m/z* 407, whose formation suggested that both hydroxylation and desulphonation processes had involved the same benzene moiety. Unfortunately, the other isomeric forms did not afforded structurally-informative losses. For 531-B no remarkable product ions were formed, while 531-C only showed a product ion at *m/z* 503 via a CO molecule loss. The isomer 531-D easily loses a water molecule (*m/z* 513).

Finally, the formation of the transformation product of *m/z* 407, that could share the same structure attributed to the previously described 531-A product ion, can be postulated to be formed via a cleavage of C-N bond with the detachment of 1,3,5-trihydroxybenzene. At high cone voltage, it afforded the loss of sulphonic group with the formation of a product ion at *m/z* 327.

Two species were formed at *m/z* 527 and could be attributed to the oxidized form of the *m/z* 531. These molecules could be the result of:

(1) the detachment of a sulphonic group, followed by hydroxylation and oxidation of a methyl to formyl group or:

(2) SO_2 detachment and oxidation of a methyl to formyl group.

For the isomer 527-B unfortunately no product ions were formed, even at high cone voltage, so that no consideration can be done. Conversely, the isomer 527-A yielded mainly a product ion at *m/z* 511, via the loss of a methane molecule, and at *m/z* 377, through the release of hydroxy ketobenzaldehyde. The latter ion formation involved the cleavage of the anthraquinone moiety and drove us to locate the hydroxy group on the anthraquinone moiety (see Scheme 3).

All the intermediate compounds detected by HPLC/MS still hold the chromophore moiety, so that the photo-bleaching cannot be linked to their formation, but could be reasonably due to the formation of smaller molecules. Conversely, GC-MS analysis showed the formation of an uncoloured compound: benzene 1,2-dicarboxylic acid, whose identification was made by using an identification program by NIST library (see Table 2). Its formation involved the cleavage of the anthraquinone moiety, which could probably occur through the mechanism proposed by Saquib and Muneer [24].

3.2.2. AV7 transformation products

Along with the dye decomposition, the formation of several intermediate compounds occurred. Four initial transformation products were identified by HPLC/MS and two secondary transformation products were detected by GC/MS. Table 3 shows the peculiar MS product ions for AV7 and all the transformation products detected by HPLC/MS. All of them had retention times shorter than AV7 and, on the basis of their *m/z* ratio and main fragments were attributed to the

structures presented below. The AV7 fragmentation study showed several peculiar losses, which are collected in Scheme 4.

In addition to the product ion at [M-2H]$^{2-}$ 260, at high cone voltage a product ion at m/z 359 was formed from the deprotonated molecule (m/z 521) via the loss of a diazo-benzenaminoacetic acid molecule. Conversely, the formation of the product ions at m/z 373 and 291 could occur from the hydrazo tautomer, through the N-N bond cleavage. These product ions will be carefully considered identifying the unknown compounds formed during the AV7 photo-induced degradation.

Two compounds at m/z 537 were detected and attributed to the hydroxyl-derivatives. Both isomers formed a product ion at m/z 307, which in a close analogy with AV7 matched with the hydroxylated form of m/z 291, formed through the combined detachment of SO_2 and 4-amino-phenylaminoacetic acid molecule. Therefore, an hydroxylation on the benzenaminoacetic acid moiety can be excluded for both isomers. In addition, the isomer 537-A yielded a product ion at m/z 507 (formaldehyde loss), that permitted to locate the OH on the methyl group. Unfortunately, 537-B did not present other peculiar losses that could help to attribute the position where the OH attack occurred.

The compound at m/z 471 was attributed to the desulphonated derivative. Its formation could be postulated to occur through the detachment of a sulphonic group and oxidation of the molecule, with the formation of the compound shown in Figure 5.

The last recognized transformation route involved the amino moiety, with the detachment of an aminoacetic group and the formation of a compound at m/z 480 (see Figure 5). Unfortunately there was no information available from MS spectra to prove which (of the two) aminoacetic group was involved in the transformation. Moreover, a support for the proposed structure might come from the GC/MS analysis, where the contemporaneous formation of the dihydroxybenzenaminoacetone and α-hydroxy naphthalene were detected (see Table 2).

The transformation products identified by HPLC/MS were still coloured, while the two products detected by GC/MS had lose the chromophore moiety and contributed to the observed photo-bleaching.

3.3. Mineralization process

Organic carbon was completely mineralized in both cases (see Figure 6 and 7). With AG25, after 1h almost 90% of the organic carbon was mineralized and underwent complete mineralization after 4 h of irradiation. Besides, AV7 mineralization slower proceeded. After 1h of irradiation 33%

of organic carbon was still present and 16h of irradiation were needed to achieve the complete mineralization.

Looking closer to the inorganic ions formation, in both cases sulphur was easier released than nitrogen. Sulphur atom was recovered as sulphate and its stoichiometric concentration was reached within 2h of irradiation for both dyes. It means that the initial transformation involved the detachment of sulphonic group in agreement with the identified intermediates presented above. Nitrogen was predominantly transformed into ammonium ions, whose formation mainly occurred after the dyes complete disappearance.

In both cases, the release of nitrogen as ammonium ions was favoured. It is particularly marked in the case of AV7, due to the presence of an amino group. It is in agreement with literature data, as it is known that tertiary and quaternary amino groups are mainly transformed into ammonium ions [33]. Conversely, as far as the degradation of the initial azo-dye was achieved, the formation of N_2 was evidenced [34, 35]. It could justify the lack in nitrogen mineralization observed for AV7.

Conclusions

Acid Violet 7 and Acid Green 25 were degraded in aqueous solution using titanium dioxide as photocatalyst. The results from this study had shown that TiO_2 mediated photocatalytic degradation was a suitable treatment to achieve not only the bleaching, but also the complete mineralization of the investigated dyes. Along with the dyes degradation, several intermediate compounds were formed during the degradation process. This study confirmed that LC-MS technique demonstrates to be a powerful tool to monitor pollutants and their related degradation compounds, even at trace level. The combined used of HPLC/MS and GC/MS allowed the identification of diverse intermediates formed at the earlier reaction steps, that involved detachment of one (or two) sulphonic group, hydroxylation, and further breakage of the dyes molecule.

References

[1] G. A. Epling, C. Lin, Chemosphere, 46(4) (2002) 561–570.

[2] Y.Z .Wang, Water Res. 34(3), (2000) 990-994.

[3] A. Mills, A Belghazi, R. H. Davies, D. Worsley, S. Morris, J. Photochem. Photobiol., A, 79 (1994) 131-139.

[4] K. Vinodgopal, P. V. Kamat, J. Photochem. Photobiol. A, 83 (1994) 141-146.

[5] C. Hachem, F. Bocquillon, O. Zahraa, M. Bouchy, Dyes Pigm., 49 (2001) 117-125.

[6] I. Arslan, I. A. Balcioglu, D. W. Bahnemann, Dyes Pigm., 47 (2000) 207-218.

[7] J. Zhao, T. Wu, K. Wu, K. Oikawa, H .Hidaka, N. Serpone, Environ. Sci. Technol., 32 (1998) 2394-2400.

[8] M. Sökmen, A. Özkan, J. Photochem. Photobiol. A, 147 (2002) 77-81.

[9] M. Vautier, C. Guillard, J. M. Hermann, J. Catal., 20 (2001) 46-59.

[10] Y. Xu, C H Langford, Langmuir, 17 (2001) 897-902.

[11] M. Muneer, R Philips, S Das, Res. Chem. Intermed., 23 (1997) 233-246.

[12] K Hirano, E Suzuki, A Ishikawa, T Moroi, H Shiroishi, M Kaneko, J. Photochem. Photobiol. A, 136 (2000) 157-161.

[13] K .Vinodgopal, I. Bedja, S. Hotechandani, P. V. Kamat, Langmuir, 10 (1994) 1767-1771.

[14] K. Rajeshwara, M.E. Osugib,W. Chanmaneec, C.R. Chenthamarakshana, M.V.B. Zanonib, P. Kajitvichyanukuld, R. Krishnan-Ayer, J. Photochem. Photobiol. C, 9 (2008) 171–192.

[15] V. A. Sakkas, Md. A. Islam, C. Stalikas, T. A. Albanis, J. Hazard. Mater., 175 (2010) 33-44.

[16] J.M. Monteagudo, A. Durán, I. San Martín, M. Aguirre, Appl. Catal. B:Environ., 95 (2010) 120-129.

[17] J. Fernández, J. Kiwi, C. Lizama, J. Freer, J. Baeza, H. D. Mansilla, J. Photochem. Photobiol. A, 151 (2002) 213-219.

[18] M.A. Fox, M.T. Dulay, Chem. Rev. 93 (1993) 341–357.

[19] D.W. Bahnemann, J. Fox, E. Pelizzetti, P. Pichat, N. Serpone, in: G.R. Helz, R.G. Zepp, D.G. Crosby (Eds.), Aquatic and Surface Photochemistry, Lewis Publ., Boca Raton, FL, 1994, pp. 261–316.

[20] I. K. Konstantinou, T. Albanis, Appl. Catal. B: Environ., 49 (2004) 1–14

[21] I. Bouzaida, C. Ferronato, J.M. Chovelon, M.E. Rammahb, J.M. Herrmann, J. Photochem. Photobiol. A, 168 (2004) 23-30.

[22] P. Calza, C. Medana, C. Baiocchi, E. Pelizzetti, Curr. Anal. Chem., 1 (2005) 267-287.

[23] W.Z. Tang, H. An, Chemosphere, 31(9) (1995) 4157-4170.

[24] M. Saquib, M. Muneer, Color. Technol., 118 (2002) 307-315.

[25] H. B. Mansour, D. Corroler, D. Barillier, K. Ghedira, L. Chekir, R. Mosrati, Food Chem. Toxicol., 9 (2007) 1670-1677.

[26] H.B. Mansour, R. Mosrati, D. Corroler, K. Ghedira, D. Barillier, L. Chekir, Environ. Toxicol. Pharmacol. 27 (2009) 231-236.

[27] I. Muthuvel, M. Swaminathan, Catal. Comm., 8 (2007) 981-986.

[28] F. Herrera, A. Lopez, G.Mascolo, P. Albers, J. Kiwi, Appl. Catal. B: Environ., 29 (2001) 147.

[29] W. Feng, D. Nansheng, H. Helin, Chemosphere, 41 (2000) 1233-1238.

[30] A. Bianco Prevot, C. Baiocchi, M.C. Brussino, E. Pramauro, P. Savarino, V. Augugliaro, G. Marcì, L. Palmisano, Environ. Sci. Technol., 35 (2001) 971-976.

[31] A. Bianco Prevot, D. Fabbri, E. Pramauro, C. Baiocchi, C. Medana, J. Chromat. A, 1202 (2008) 145-154.

[32] M. Holcapek, P. Jandera, P.Zderadicka, J. Chromatogr. A 926 (2001) 175–186.

[33] K. Nohara, H. Hidaka, E.Pelizzetti, N. Serpone, J. Photochem. Photobiol. A, 102 (2-3) (1997) 265-272.

[34] C. Guillard, H. Lachheb, A.Houas, M. Ksibi, E. Elaloui, J.M.Herrmann, J. Photochem. Photobiol. A, 158 (2003) 27-36.

[35] P. Calza, E. Pelizzetti, C. Minero, J. Appl. Electrochem., 35 (2005) 665-673.

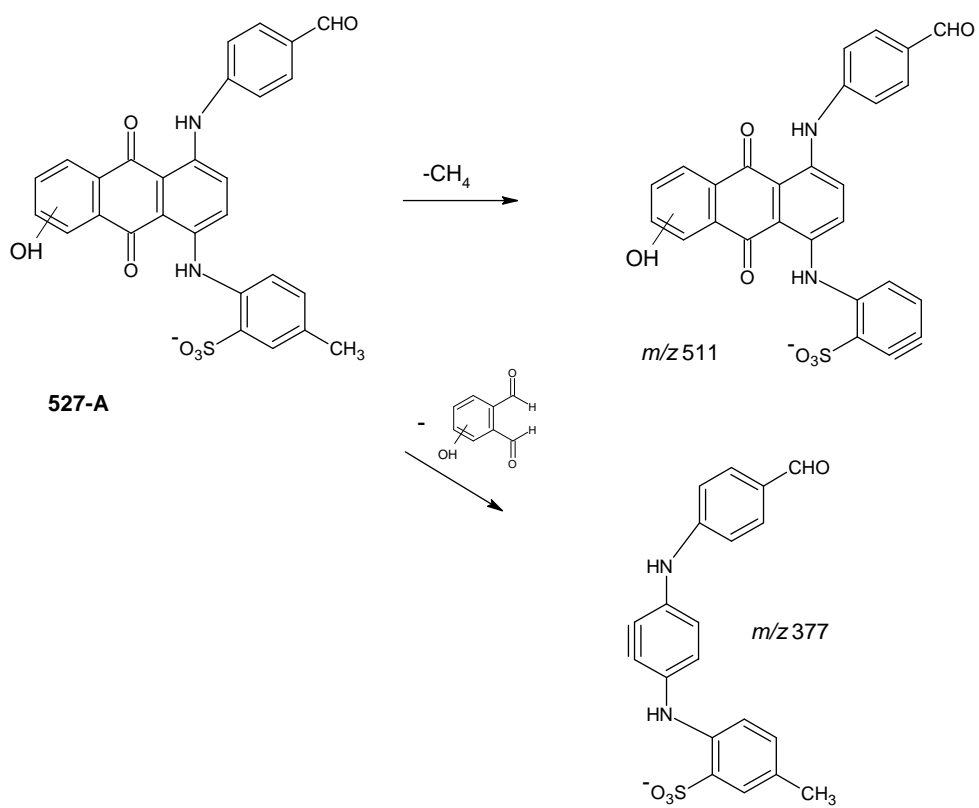**Scheme 1**. Key fragmentation pathways followed by 513-B and C.

m/z 328

513-B

m/z 408

513-C

m/z 435
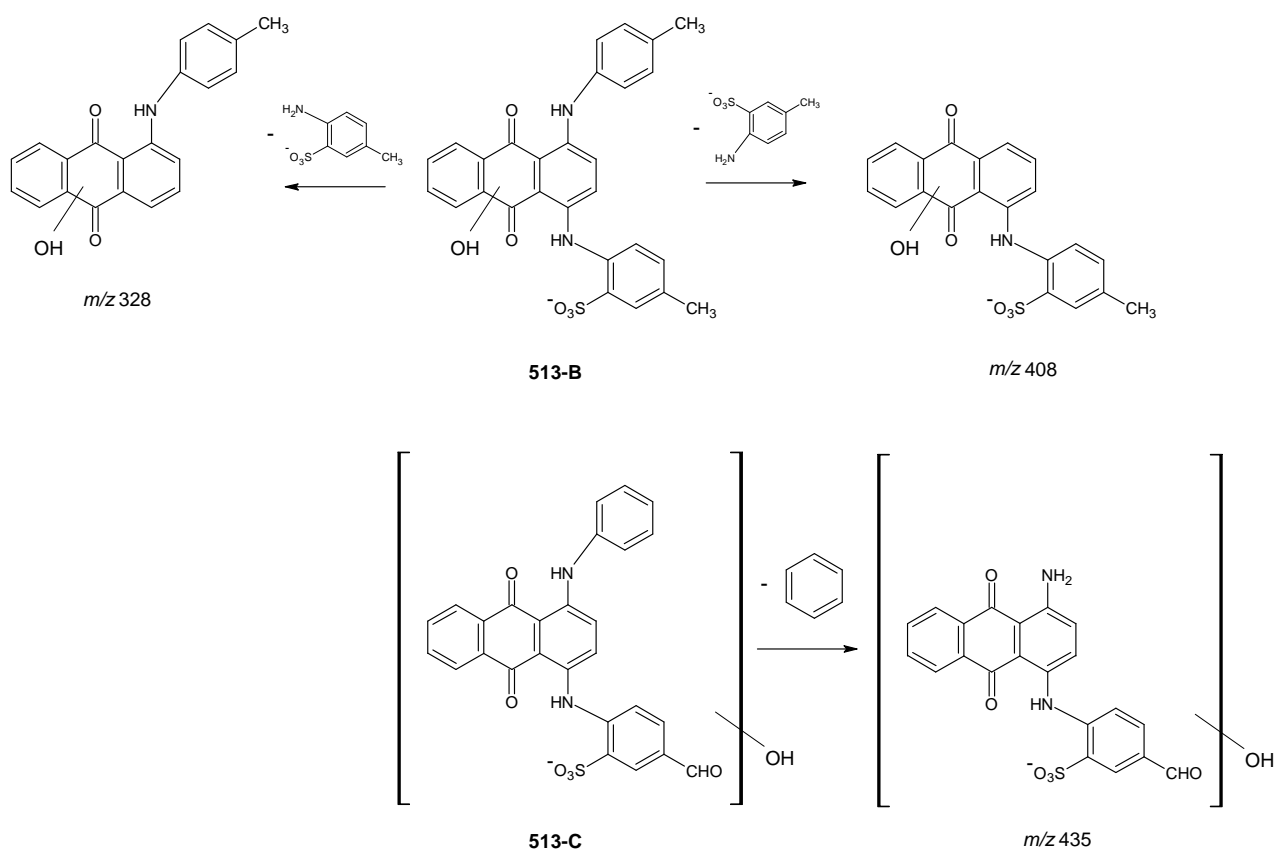
Scheme 2. Key fragmentation pathways followed by 531-A.

531-A   *m/z* 407
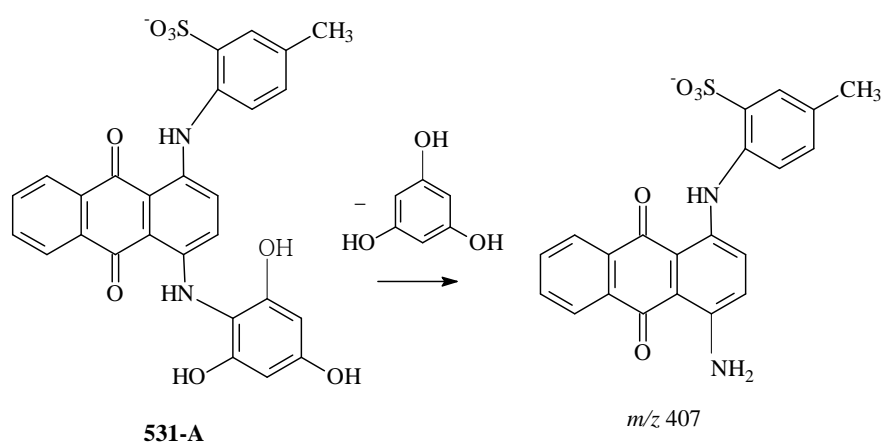
Scheme 3. Key fragmentation pathways followed by 527-A.

Scheme 4. Key fragmentation pathways followed by AV7.

m/z **521**

m/z 373   -H₂SO₃
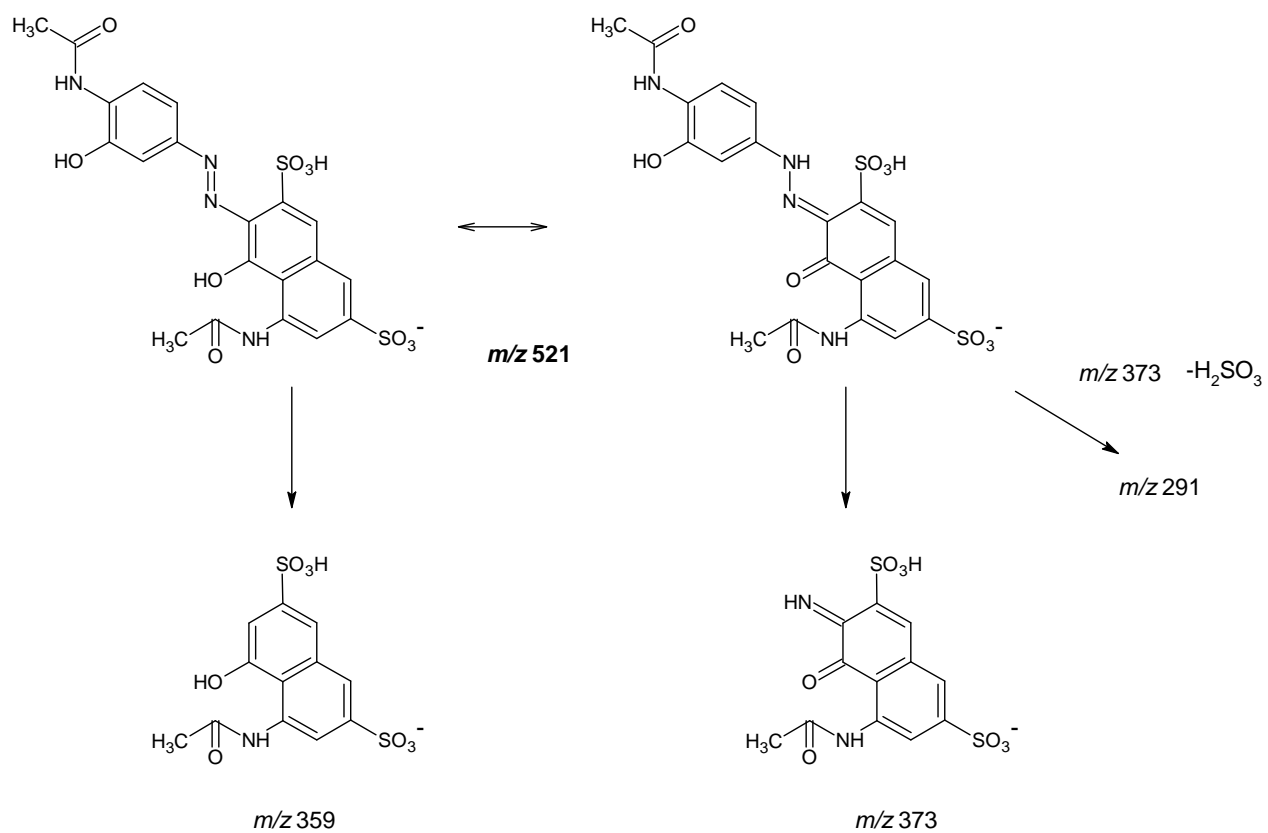
m/z 291

m/z 359

m/z 373

Figure captions

Figure 1. Structure of AG25 and AV7.

Figure 2. Degradation of AG25 20 mg L^{-1} as a function of the irradiation time in sterilized water or TiO$_2$ suspension (200 mg L^{-1}).

Figure 3. Degradation of AV7 20 mg L^{-1} as a function of the irradiation time in sterilized water or TiO$_2$ suspension (200 mg L^{-1}).

Figure 4. MS spectrum at 70 cone voltage for 591-C and proposed fragments after 5 minutes of irradiation.

Figure 5. Structure for the intermediate compounds at m/z 407 e 480.

Figure 6. Degradation of AG25 20 mg L^{-1} as a function of the irradiation time in TiO$_2$ suspension (200 mg L^{-1}): TOC disappearance, sulphate, nitrate and ammonium evolution as a function of the irradiation time.

Figure 7. Degradation of AV7 20 mg L^{-1} as a function of the irradiation time in TiO$_2$ suspension (200 mg L^{-1}): TOC disappearance, sulphate, nitrate and ammonium evolution as a function of the irradiation time.
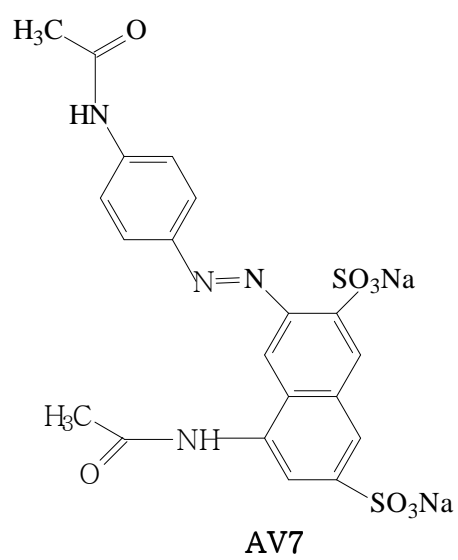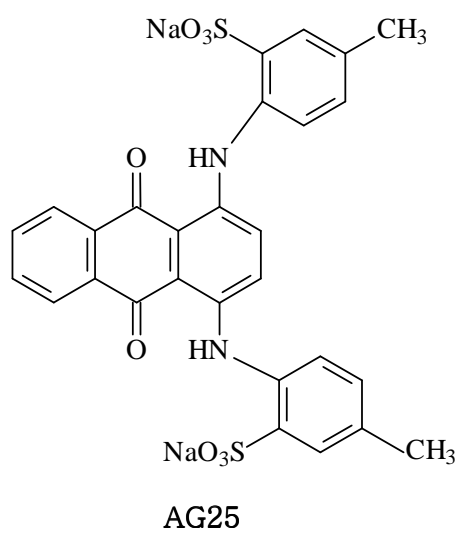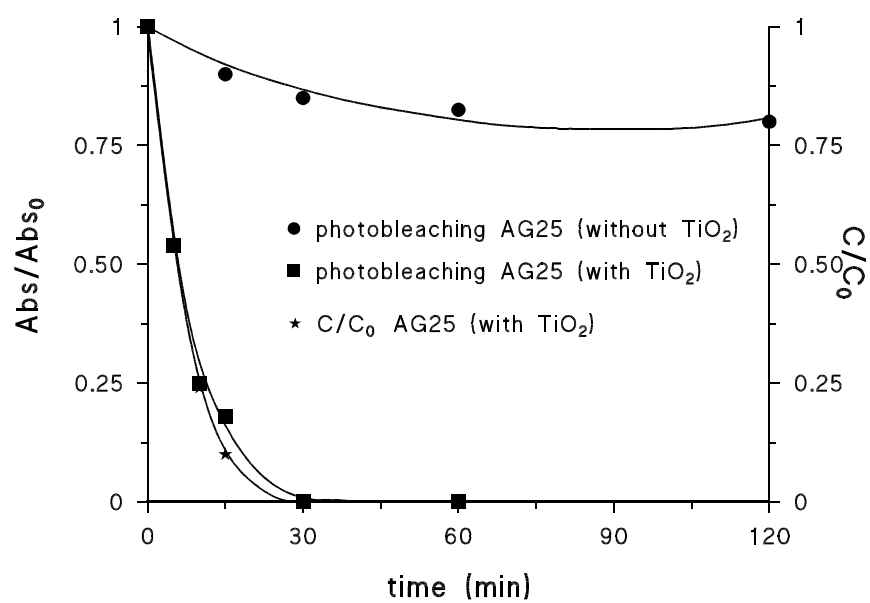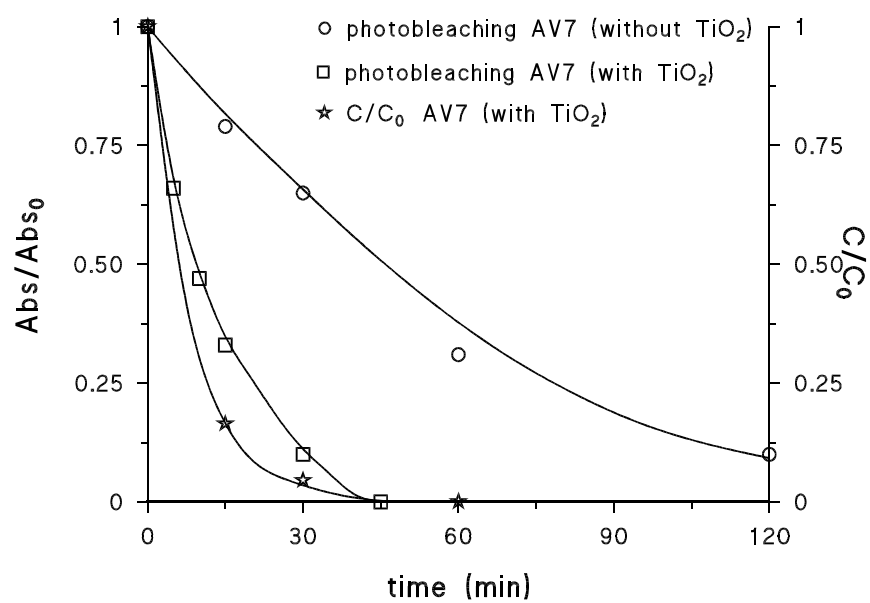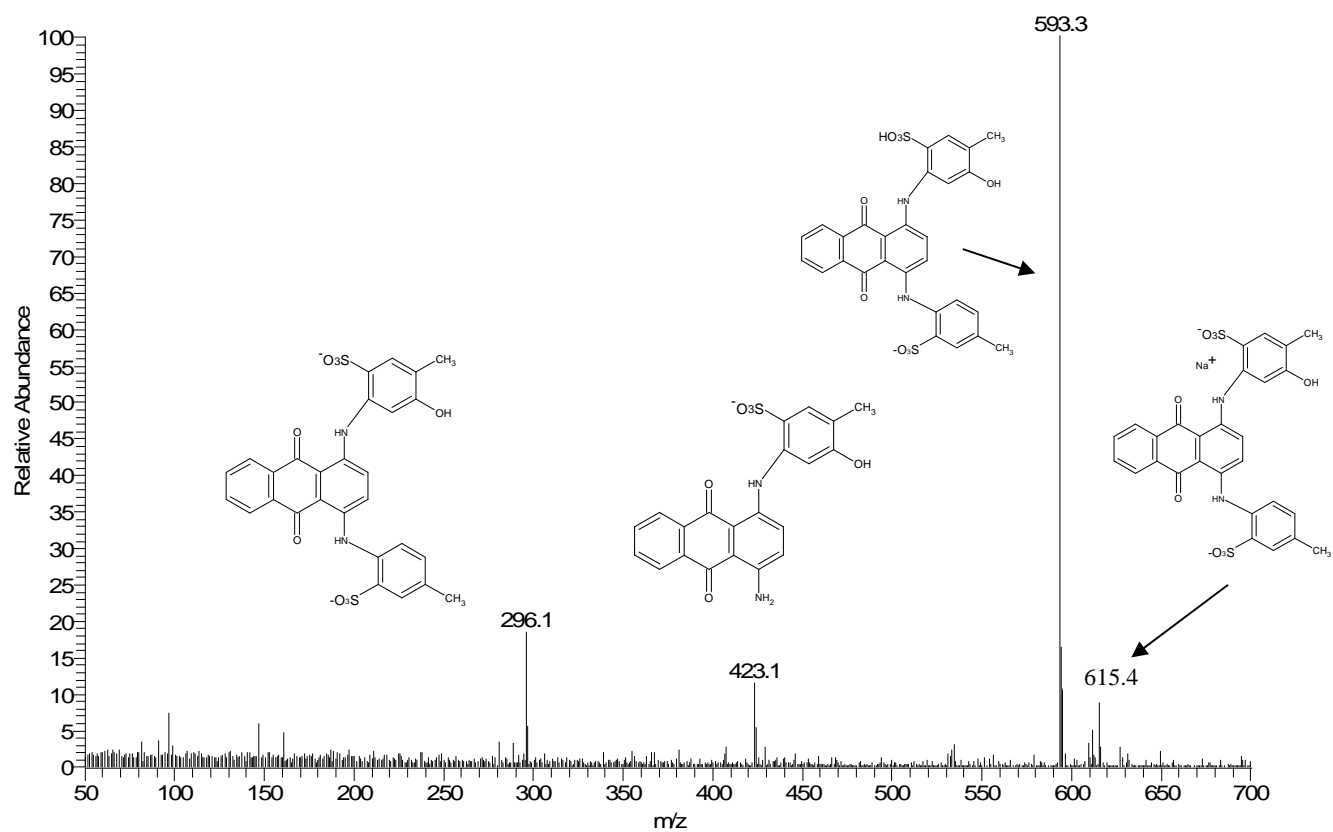
Figure 1

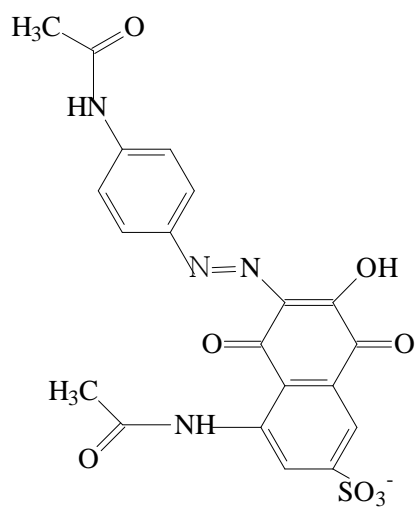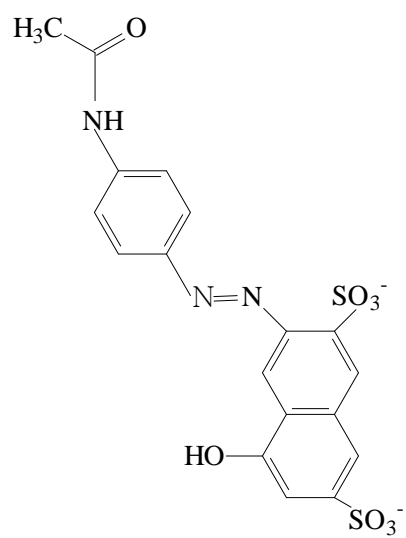

AG25

AV7

Figure 2

Figure 3

Figure 4

Figure 5

m/z 471
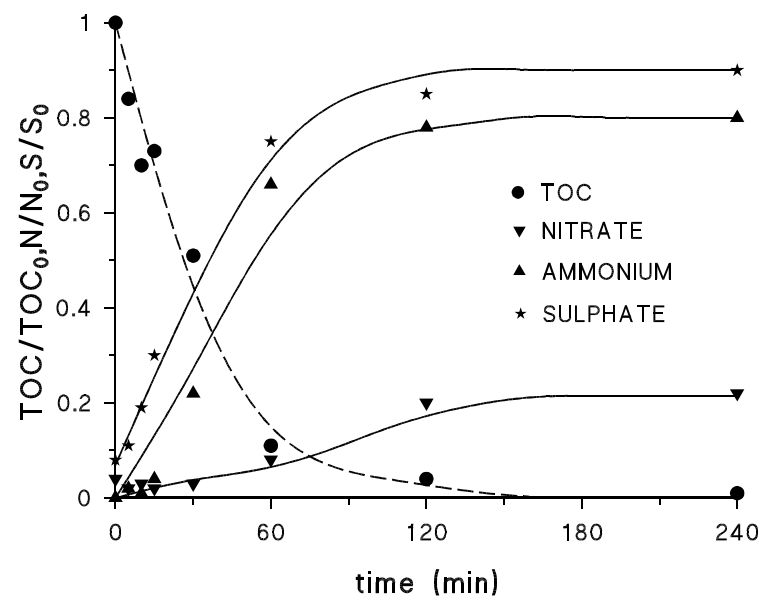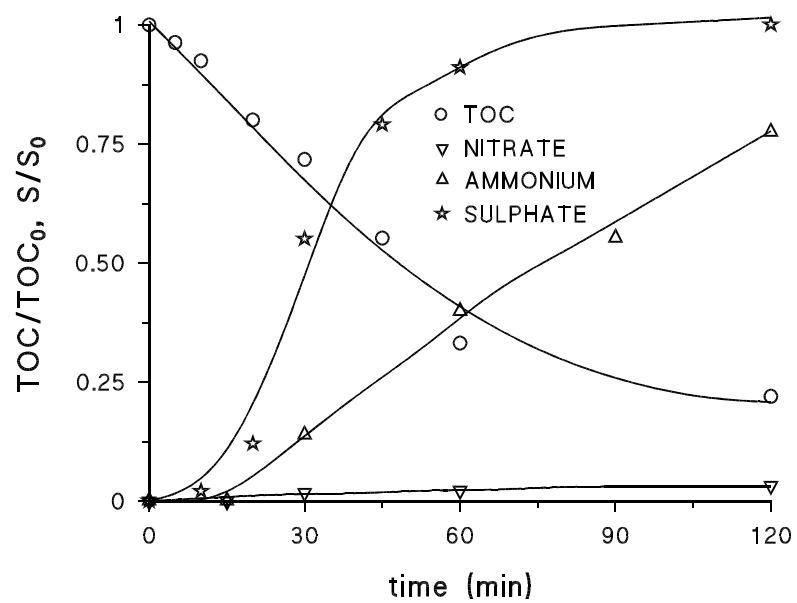

m/z 480

Figure 6

Figure 7

Table 1. Intermediate compounds formed from AG25 transformation (at AG25 half life time) and detected by HPLC/MS.

m/z	t_R (min)	Cone voltage	Product ions
577	23.05	30	678 (62), 577 (52), 288 (100)
		70	577 (100), 288 (74)
		100	577 (100)
513-A	24.67	30	513 (20), 413 (100), 369 (24)
		70	543 (10) ,513 (100) ,369 (20) ,169 (16)
		100	-
513-B	24.94	30	513 (8), 408 (10)
		70	513 (88), 408 (100)
		100	513 (70), 430 (22), 408 (100), 328 (48)
513-C	25.80	30	513 (100), 435 (26)
		70	513 (100), 435 (26)
		100	513 (100), 435 (68), 79 (40)
513-D	26.38	30	513
		70	513
		100	513
513-E	26.91	30	513
		70	513 (100), 495 (20), 325 (40), 293 (8), 239 (64)
		100	513 (100), 325 (36), 293 (32)
593-A	20.51	30	593 (100)
		70	593 (100), 296 (14), 615 (10)
		100	-
593-B	21.69	30	-
		70	593 (100), 296 (16), 615 (10)
		100	615 (30), 593 (100)
593-C	21.93	30	-
		70	593 (100), 615 (10), 423 (12), 296(20)
		100	615 (12), 593 (100)
593-D	22.11	30	-
		70	593 (100), 591 (70), 296 (20), 615 (10)
		100	-
611-A	20.22	30	-
		70	611 (100), 633 (Na) (12), 579 (20), 305(14), 161 (28)
		100	-
611-B	21.08	30	-
		70	611(100), 593 (14), 305 (10)
		100	611 (100), 633 (28)
407	23.42	30	407 (100)
		70	407 (100), 296 (4)
		100	407 (100), 327(14)
531-A	24.09	30.	531 (12), 407 (100)
		70	531 (8), 407 (100)
		100	531 (6), 407 (100)
531-B	24.83	30	531 (100)
		70	543 (6), 531 (100), 515 (26)
		100	-

531-C	25.52	30	-
		70	531 (100), 503(78), 430(48), 221 (40)
		100	-
531-D	26.01	30	-
		70	531(14), 513(22), 265 (100)
		100	265 (100), 513 (22)
527-A	25.67	30	527(100), 511(14)
		70	549(4), 527(100), 511(12)
		100	549 (2), 527(100), 511(6), 377(8)
527-B	26.17	30	-
		70	-
		100	-

Table 2. . Intermediate compounds formed from AG25 and AV7 transformation and detected by HPLC/MS.

Compound	t_R (min)	Ions (m/z)
Benzene- 1,3-dicarboxylic acid (AG25)	13.45	121; 149; 166
α-hydroxy naphthalene (AV7)	15.50	115; 144
Dihydroxybenzenamino acetone (AV7)	18.27	138; 152; 167

Table 23. Intermediate compounds formed AV7 transformation (at AV7 half life time) and detected by HPLC/MS. In round brackets are shown the relative ion abundances.

m/z	t_R (min)	Cone voltage	Product ions
521	18.52	40	521 (100), 260 (20)
		70	521 (100), 291 (8)
		100	521 (100), 373 (4), 359 (18), 291(89)
471	20.58	40	471 (100)
		70	471 (100)
		100	471 (100)
480	18.37	40	-
		70	480 (100)
		100	480 (100)
537-A	17.39	40	537 (100)
		70	537 (100)
		100	537 (100), 507 (25), 307(90), 265 (40)
537-B	18.78	40	537 (100)
		70	537 (100)
		100	537 (100), 457 (20), 307 (50)